

# Exploration of Boron Nitride

By Louis Baum

Department of Physics and Astronomy, University of California at Los Angeles

August 31 2012

Atomically thin crystals have recently been the topic of much study due to the availability of high quality crystal samples produced by mechanical exfoliation. Some notable examples of these crystals are graphene and boron nitride. Graphene is a single sheet of carbon atoms arranged in a honeycomb lattice. These sheets are a basic component of other carbon structures such as buckyballs, carbon nanotubes, and graphite. Boron nitride, often called white graphene, has a similar structure, a single sheet of boron and nitrogen atoms arranged in a honeycomb lattice. These materials have been used extensively for the testing of relativistic quantum mechanics and low temperature thermodynamics. In addition, these materials are suited for applications in nano-scale production of transistors and other electronic devices.

These thin quasi-two dimensional crystals also allow for the testing of the theoretical description of crystals described by Peierls and Landau.<sup>1,2</sup> Fluctuations in position due to zero point and thermal motion that are compounded with crystal size forbid the existence of a one dimensional crystal. Three dimensional crystals are stable at low temperatures, and have a melting point where thermal motion causes the regular crystal lattice to break down. Stable two dimensional crystals were excluded in the thermodynamic limit by Mermin in 1968.<sup>3</sup> However, the small size of real crystal samples leads to concerns that the thermodynamic limit is not appropriate to characterize these crystals. An

experimental study has used the electron diffraction pattern of graphene to measure the Debye Waller factor, a measure of the mean square displacement of atoms from their ideal lattice positions.<sup>4</sup> By extending this technique to measure the Debye Waller factor of monolayer boron nitride we hope to refine our understanding of the structure of these quasi-two dimensional materials.

Confirmation of the structure of these materials is impossible with optical microscopy. The diffraction limit, given by  $d = \frac{\lambda}{2N.A.}$ , limits the resolution of optical microscopy. Since optical light has wavelengths around  $\lambda \approx 550nm$ , a typical numerical aperture is  $N.A. \approx .5$  and the interatomic spacing is only  $0.142nm$ <sup>5</sup>, direct observation of the structure of these crystals is far beyond the resolution limit of optical microscopy. Electron microscopy is used to resolve these structures because an electron has a De Broglie wavelength given by

$$\lambda = \frac{hc}{\sqrt{KE^2 + 2KE m_0 c^2}}$$

We use an acceleration potential of 80 keV because higher electron energies lead to sample destruction and deterioration.<sup>6,7</sup> At 80 keV the electron wavelength is approximately 4 pm. However, the spatial resolution of electron microscopes is limited by spherical aberration as opposed to the diffraction limit. Spherical aberration is caused by changes in refraction when electrons interact with the edges of a lens as opposed to the center of the lens. Many Electron Microscopes have spherical

aberration correctors, however the Titan 80-300 kV S/TEM (transmission electron microscope) used for this research does not. The Titan TEM can achieve lattice resolution which is approximately 0.1 nm.

The short wavelength of electrons in the TEM permits the use of electron diffraction to image crystals and lattice structure. Crystals are regular arrangements of atoms where transitions between like atoms can be described with any linear combination of translation vectors. Boron nitride is a hexagonal crystal with two dimensional transition vectors  $a_1$  and  $a_2$  depicted in Figure 1. Electron diffraction produces an image that is in reciprocal space, where reciprocal lattice vectors are defined as

$$b_1 = \frac{a_2 \times a_3}{a_1 \cdot (a_2 \times a_3)}$$

$$b_2 = \frac{a_3 \times a_1}{a_1 \cdot (a_2 \times a_3)}$$

Linear combinations of reciprocal vectors describe all points on the boron nitride reciprocal lattice.

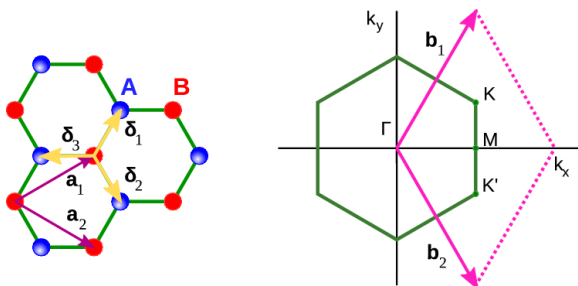


**Figure 1.**<sup>8</sup> Left: the hexagonal structure of boron nitride with depicting vectors  $a_1$  and  $a_2$ . Boron atoms are depicted in red and Nitrogen atoms are depicted in blue. Right: Reciprocal space diagram of boron nitride with reciprocal lattice vectors  $b_1$  and  $b_2$ .

The crystal structure of boron nitride can be confirmed by taking a

diffraction pattern and studying the distance between the peaks. The distance between diffraction peaks is a value with units of  $\frac{1}{meters}$  and by calibrating this distance with a known sample the length of a B-N bond can be calculated.

The relative intensities of the diffraction peaks are proportional to the squared modulus of the structure factor for the material.<sup>9</sup> The structure factor represents the scattering contribution for each atom in the crystal and this factor is summed up over all atoms in the crystal. The equation for the structure factor is presented below.<sup>10</sup>

$$f(\Delta k) = \sum_{Lattice} e^{-i(\Delta k \cdot R_l)} \sum_{Basis} e^{-i(\Delta k \cdot R_b)} \left( \frac{\gamma m}{2\pi \hbar^2} \right) \int e^{-i(\Delta k \cdot r')} V(r') d^3 r'$$

The above equation can be schematically represented as:

$$f(\Delta k) = S_l S_b F_{atom}(\Delta k)$$

Where  $F_{atom}(\Delta k)$  is the atomic form factor, which represents the scattering contribution of each atom,  $S_l$  and  $S_b$  are sums that account for all atoms in the crystal.

Through simplification of this equation it is possible to identify that the diffraction pattern for boron nitride is dependent on whether there are an even or an odd number of layers  $N$ . In addition, for any number of layers there are both strong and weak peaks. The following chart depicts the relative intensity of the peaks, without giving consideration to the exponential decay due to thermal motion or the variation of the atomic form factor with scattering angle.

	Strong Peaks	Weak Peaks
Even	$N (F_b + F_n)^2$	$\frac{1}{4} N (F_b + F_n)^2$
odd	$(N - 1)(F_b + F_n)^2 + F_b^2 - F_n^2 + 4F_n^2$	$\frac{1}{4}(N - 1)(F_b + F_n)^2 + F_b^2 - F_n^2 + 4F_n^2$

**Table 1:** Relative intensity of diffraction pattern peaks as a function of atomic form factor F and number of layers N.  $F_b$  and  $F_n$  correspond to the scattering contributions from boron and nitrogen atoms respectively.

Mechanical exfoliation produces relatively large defect free crystals of boron nitride. Placing crystal samples on a substrate of thin  $\text{SiO}_2$  maximizes the optical contrast between the substrate and a single layer of boron nitride. The graph in Figure 2 illustrates the optical contrast of boron nitride on a  $\text{SiO}_2$  layer as a function of layer thickness as well as the wavelength of light. We used a layer of 90nm of  $\text{SiO}_2$  to maximize the optical contrast for white light with an average wavelength of 550 nm.

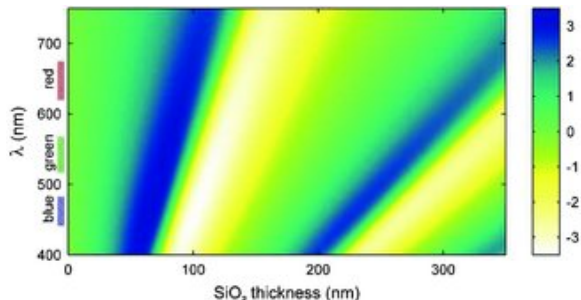


**Figure 2:**<sup>11</sup> Optical contrast as a function of wavelength of light and substrate thickness for light incident on boron nitride.

Throughout the summer we were unable to locate a monolayer large enough to characterize with electron diffraction. This was primarily due to significantly lower optical contrast of boron nitride compared to similar monolayer crystals such as graphene. In addition, I believe that true monolayer samples occurred with less frequency because the inter-planar bonds of boron nitride are stronger than those of

graphene.<sup>12</sup> Attempts to increase the contrast of monolayer boron nitride include the use of tinted filters, adjusting digital camera parameters and varying the thickness of the  $\text{SiO}_2$  substrate layer. The use of filters was abandoned because no substantial gains in contrast were recognized and the filter impeded the identification of thicker sample of boron nitride. Adjusting the digital camera parameters was also discontinued because differentiation between tape residue and thin boron nitride increased in difficulty dramatically. Lowering the  $\text{SiO}_2$  substrate thickness from 300nm to 90nm improved optical contrast for thin regions of boron nitride as you can see from the difference in the highlighted areas of two chips presented in Figure 3.

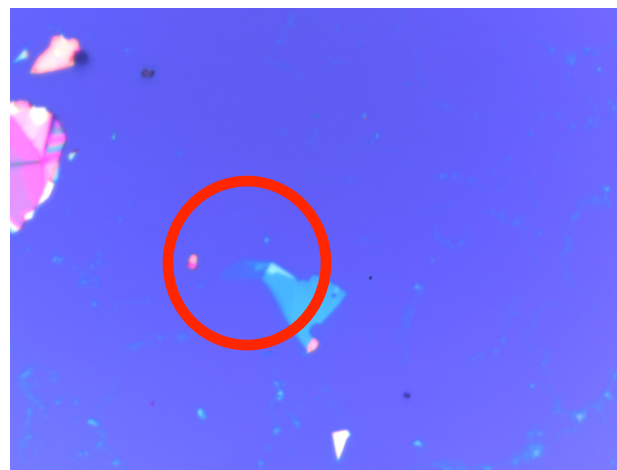
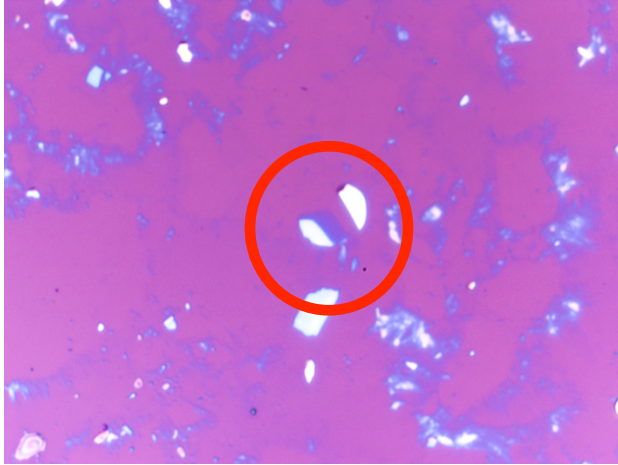


**Figure 3:** Above: A thin flake of boron nitride on 300nm  $\text{SiO}_2$ . Below: A thin flake of boron nitride on 90nm  $\text{SiO}_2$ . Red regions indicate regions of interest.



The use of Raman spectroscopy was considered due to citations from the literature indicating its successful use as an identification tool.<sup>10</sup> However, consulting with peers made it clear that Raman spectroscopy was a time intensive process and required samples much larger than samples we could readily identify as potentially single layer. Raman spectroscopy was never attempted.

After samples had been identified as potentially thin, they were transferred to an over-etched window or TEM grid for further imaging and electron diffraction in the electron microscope. The transfer process to the over-etched chip began by spin coating the sample with poly(methyl methacrylate) (pmma). We then scraped the pmma from unwanted areas. We proceeded to etch the pmma free in a 1 M solution of NaOH. Next, we used probes to position the crystal sample over the window. Finally, once the crystal was in position the pmma was removed by dissolving it with a drop of dilute pmma solution. The chip was immediately cleansed of residual pmma in an acetone wash followed by isopropyl alcohol and blown dry with nitrogen gas. This transfer process is still under development and

while it is effective, there is a significant failure rate. The two stages with the highest failure were the etching stage, where the sheet of pmma could curl up in solution or simply become lost, and the removal stage, which would often result in the crystal sample being completely washed away or damaged.

The use of two different types of support structures to image samples in the TEM was due to convenience rather than design. The TEM grids were vastly superior to the over-etched window chips. A TEM grid mounted sample allowed a much larger area to be visible in the TEM, this allowed multiple target areas to be selected and investigated.

To continue this work optical identification of monolayer samples should remain a priority. The ability to observe samples with a 100x objective with a numerical aperture of .9 would be a boon to an investigator. Additionally, we would advocate the continued use of 90nm SiO<sub>2</sub> which provided substantially better contrast compared with samples mounted on 300nm SiO<sub>2</sub>. A final thought would be that the use of TEM grids to mount samples is a vastly superior process relative to mounting prospective thin boron nitride on over-etched windows. These steps should improve the chances of finding a useable boron nitride sample to allow for electron diffraction and an eventual measurement of the Debye-Waller factor.

#### Acknowledgements

I would like to extend thanks to Billy Hubbard for his patience and guidance over the course of this work. Thanks to Professor Regan for welcoming me to the research team and providing needed advice and

assistance throughout the summer. I would also like to recognize Ed White and Louis Yang for their cooperative efforts. This work was made possible by funding provided by the NSF REU program. Finally, I would like to thank Francoise Queval for her hard work organizing the REU program.

---

<sup>1</sup> L. D. Landau, E. M. Lifshitz, L. P. Pitaevskii, J. B. Sykes, and M. J. Kearsley, *Statistical physics. Part 1* (Butterworth-Heinemann, Amsterdam, 2003).

<sup>2</sup> R.E. Peierls, *Helv. Phys. Acta* 7, 81 (1934) as translated in R.E. Peierls and R.H. Dalitz, *Selected scientific papers of Sir Rudolf Peierls : with commentary* (World Scientific, Singapore, 1997).

<sup>3</sup> N. D. Mermin, *Physical Review* 176, 250 (1968).

<sup>4</sup> B. Shevitski, M. Mecklenburg, W. A. Hubbard, E. R. White, B. Dawson, M. S. Lodge, M. Ishigami, and B. C. Regan. *Dark-field transmission electron microscopy and the Debye-Waller factor of graphene* (submitted for publication)

<sup>5</sup> Raji Heyrovska (2008). "Atomic Structures of Graphene, Benzene and Methane with Bond Lengths as Sums of the Single, Double and Resonance Bond Radii of Carbon". arXiv:0804.4086 [physics.gen-ph]

<sup>6</sup> B.W. Smith and D.E. Luzzia, *Journal of Applied Physics* 90(7), 3509 (2001).

<sup>7</sup> A. Zobelli A. Gloter C.P. Ewels G. Seifert and C. Colliex, *Physical Review B* 75 (2007).

<sup>8</sup>

<http://oer.physics.manchester.ac.uk/AQM2/Notes/Notes-6.4.html#fig:Rel:graphene2>

<sup>9</sup> Kittel C, *Introduction to Solid State Physics*, 1st ed. 1953 - 8th ed. 2005

<sup>10</sup> B. Fultz and J. M. Howe, *Transmission electron microscopy and diffractometry of materials* (Springer, Berlin; New York, 2008).

<sup>11</sup> R. V. Gorbachev et al., *Hunting for monolayer Boron Nitride: optical and Raman signatures. Small* 7, 465 (2011).

<sup>12</sup> D. Pacilé, J. C. Meyer, Ç. Ö. Girit, and A. Zettl, *Appl. Phys. Lett.* **92**, 133107 \_2008\_.